FAILURE OF POLYAMIDE 12 NOTCHED SAMPLES MANUFACTURED BY SELECTIVE LASER SINTERING

M. Crespo, T. Gómez-del Río, J. Rodríguez

DIMME, Grupo de Durabilidad e Integridad Mecánica de Materiales Estructurales, Universidad Rey Juan Carlos, Escuela Superior de Ciencias Experimentales y Tecnología, C/ Tulipán, s/n. Móstoles, 28933 Madrid, España.

FAILURE OF POLYAMIDE 12 NOTCHED SAMPLES MANUFACTURED BY SELECTIVE LASER SINTERING

M. Crespo, T. Gómez-del Río, J. Rodríguez

DIMME, Grupo de Durabilidad e Integridad Mecánica de Materiales Estructurales, Universidad Rey Juan Carlos, Escuela Superior de Ciencias Experimentales y Tecnología, C/ Tulipán, s/n. Móstoles, 28933 Madrid, España.

ABSTRACT

Fracture resistance of polyamide 12 was measured with tensile tests on notched specimens with different notch tip radii. The specimens were processed by additive manufacturing techniques and the tests were carried out in two different orientations to evaluate the potential anisotropy of the material. Finite element analysis was performed to know the stress state of the whole specimen. Then, the failure of the specimens were described using the theory of critical distances. The influence of possible manufacturing defects in the material were incorporated using a probabilistic approach, associated with a Weibull distribution. A fractographic analysis of the post-mortem specimens allowed to identify those mechanisms responsible for the material failure in each orientation.

KEYWORDS

Polyamides, fracture toughness, notches, additive manufacturing

1. INTRODUCTION

Additive manufacturing techniques differ essentially from traditional subtractive manufacturing because samples are built in a layer-by-layer manner from a computer prototype using digitally controlled and operated machines [1]. One of the main advantages is the rapid transition from the design phase to the final part, thus facilitating the replacement in many cases of long and complicated processes of numerically controlled machining. This greater adaptability is also a profit when small modifications in the pieces have to be done in the final stages of machining [2]. There are different additive manufacturing techniques, using filaments or powder as the initial state of the polymer used. Among them, Selective Laser Sintering (SLS) uses a laser as the power source. The laser scans automatically the space, binding the material at those points indicated in the 3D model, creating the final solid structure.

The polymeric materials that are commonly used with the SLS technique are PEEK, PC and PA12. The use of polyamide 12 is very widespread in the field of additive manufacturing through SLS, with a market share of 95%. Mainly due to its ease of

forming, to have a large thermal window processing, and its low price compared to other materials used with this technique [3-4].

The mechanical response of additive manufactured pieces depends on the type of technique used, but also on the printing direction. Because of the layer-by-layer assembling process, anisotropy is inherent to this type of materials. The mechanical behavior can be considered isotropic inside the layers, but it may be weaker across them [5]. Of course, the final behavior will depend on the parameters used during the manufacturing process: laser power (i.e., energy supplied to melt the powder), the spacing and the thickness of the layers, etc. These parameters optimization would reduce imperfections as pores, presence of un-melted powder particles, gasses retention and gaps between the layers. Nevertheless, discontinuities and defects are inevitable and they may control the mechanical failure of the final piece, acting as stress concentrators, when they become cracks or pores. The initial design may probably include also sudden changes in geometry. In order to analyze the influence of all these defects or stress concentrators, tests are performed on notched specimens, whose behavior is in between that of the smooth specimens, which can be described by the Mechanics of Materials, and that of the cracked specimens, object of study of the Fracture Mechanics.

The prediction of the failure loads of notched specimens, would be wrong if it is calculated directly using the Fracture Mechanics Theory, i.e., considering notched samples as specimens with a sharp crack [6]. The behavior of notched samples can be easily analyzed using the Theory of Critical Distances (TCD). The easy version of this theory predicts the failure of a notched specimen when the stress reaches a critical value, σ_0, at a critical distance from the tip of the notch, L [7]. Combining TCD and the elastic stress field at the end of the notch described by the Creager-Paris equation, the material fracture toughness can be obtained from the failure loads of notched samples [8-10].

This work deals with the influence of the printing direction on the failure loads of SLS polyamide 12 notched samples. Tensile mode tests of notched samples with different tips radii were performed and the fracture surfaces were analyzed by scanning electronic microscopy (SEM) with the aim of study the failure mechanisms.

2. METHODOLOGY

2.1. Materials and samples

The material studied in this work is a neat polyamide 12 (PA12) manufactured by Prodintec from PA2200 powders. The original powder has a bulk density $\rho > 0.430$ g/cm^3 and a mean grain size of 58 μm (d50 measured by laser diffraction).

Specimens were prepared by SLS, using a unit EOS Formiga P100 from FUNDACION PRODINTEC, Gijón, Spain, where manufacturing parameters were optimized. These parameters vary even using the same manufacturing unit, with changes in the finished products between some manufacturers and others [11].

The geometry of the specimens was designed to be tested in tensile mode, passing from a cylindrical geometry, with threads for the transmission of load, to a prismatic geometry

in the central zone with rectangular cross section (40 mm in length, 7.5 mm in width and 3 mm in thickness). Notches with different tip radii (0.2 mm, 0.5 mm, 0.8 mm and 1 mm) were introduced as indicated in the example of Figure 1. The whole shape of the samples is directly performed by the SLS manufacturing process, even the tip radius, without post machining, avoiding so the eventual damage caused in this kind of processes.

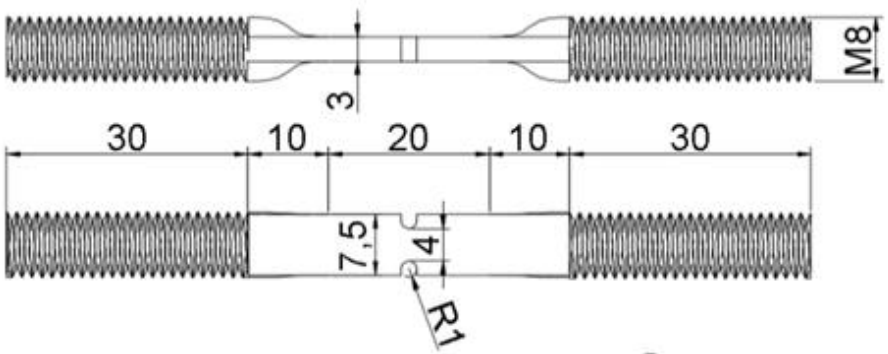

Figure 1. Sample geometry with 1 mm notch tip radius.

Two different sample batches were prepared, each one manufactured in a different printing orientation. First batch was made with the deposition direction parallel to the tensile force in the mechanical test, and the second batch printing orientation was perpendicular to the axis of the force applied in tests. These two different manufacturing orientation samples were named 0º and 90º, respectively. Figure 2 shows a schematic draw of both orientations.

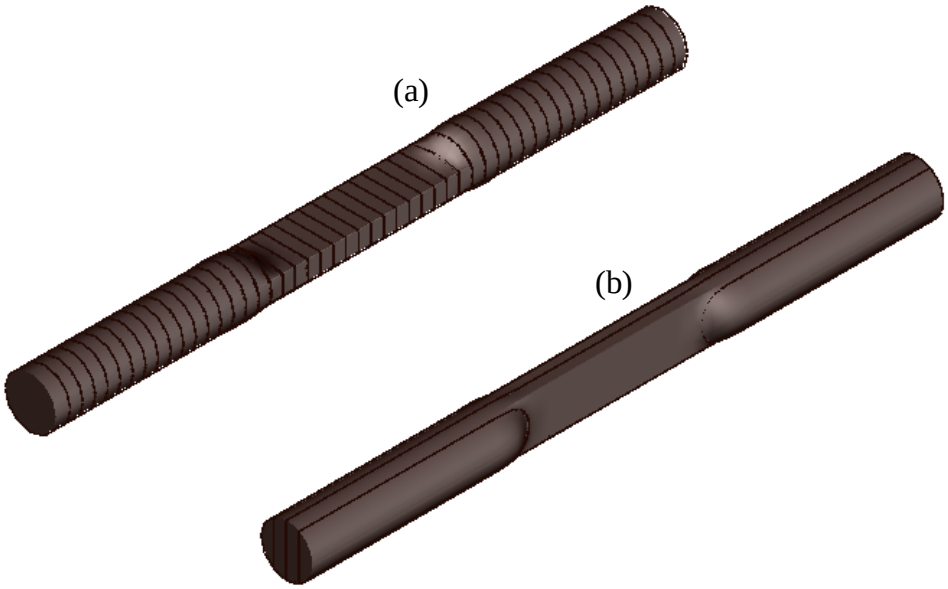

Figure 2. Schematic draw showing the direction of the printed layers by SLS additive manufacturing technique: a) perpendicular and b) parallel to the force applied during the tensile test.

Sharp cracks were manually introduced in some tensile specimens to measure the fracture toughness of the PA12. The crack was generated by sliding a razor blade with a 3 μm

radius at the edge (Figure 3). Sharp cracks performed had a tip radius lower than 20 μm and a length of 2.7 mm.

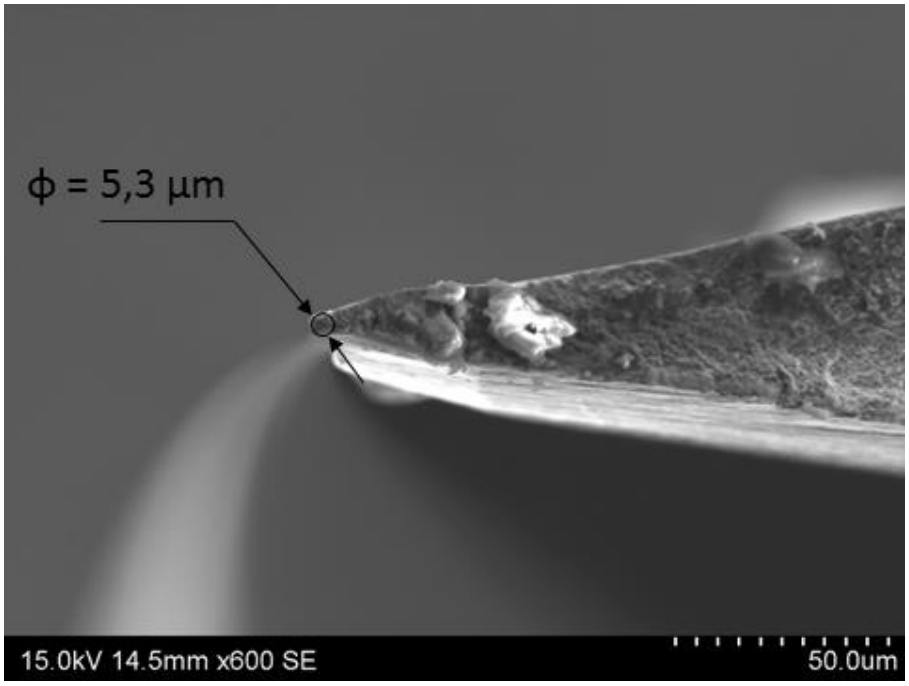

Figure 3. Sharp crack tip radius obtained by sliding notch sharpening procedure.

2.2. Mechanical tests

Low rate tensile tests were carried out in an electromechanical testing machine (MTS RF/100) with a load cell of 5 kN, following the ASTM 638-03 [12] guidelines and with a cross head speed of 2 mm/min. Displacements in the specimens were measured using a LIMESS videoextensometer by digital image correlation (DIC) (Figure 4).

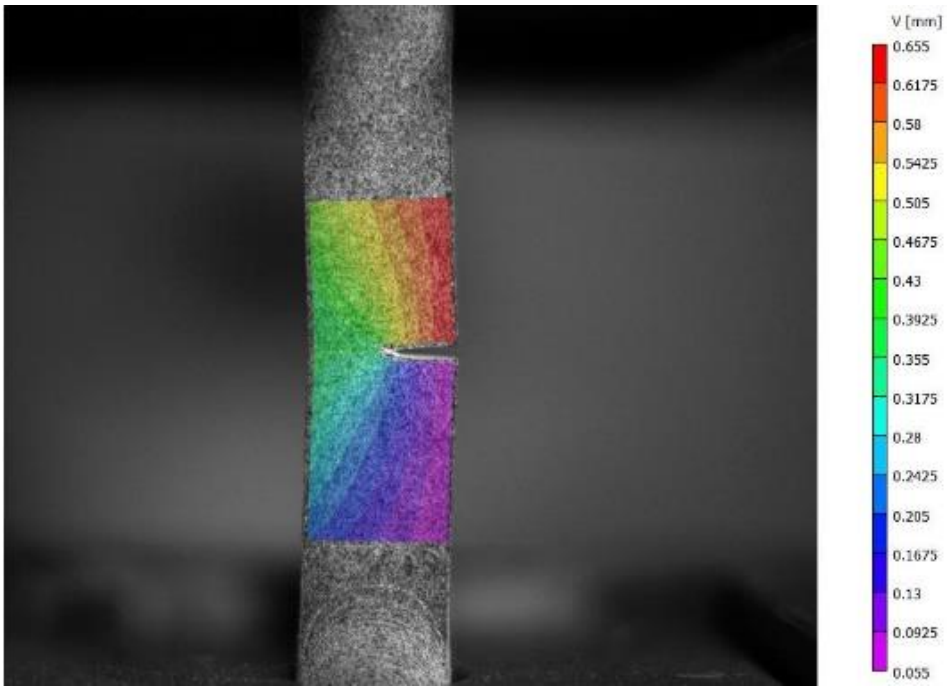

Figure 4. Displacement field measured by DIC in a notched sample.

2.3. Fractography

The fracture surfaces of the SLS specimens were inspected using scanning electron microscopy (SEM) to determine the micromechanisms of failure and, particularly, the existence of defects that could influence the results obtained. The fracture surfaces were gold coated to enhance their conductivity and were examined using a SEM HITACHI S3400N.

2.4. Finite element method (FEM) analysis

In a first approximation to apply the TCD, the elastic stress fields in the samples were determined by finite element modelling using the commercial program ANSYS.

The symmetry allows the modelling of only half sample. The analyses were carried out under plane stress conditions. Bulk elements are conventional quadrilaterals with four integration points. The material constitutive equation was that corresponding to a linear elastic behavior with a Young's modulus of 1.6 GPa and Poisson ratio of 0.4. A displacement ramp is applied to one end of the specimen while the other end is fixed. The reaction force at the fixed end is used to identify failure. The stress field around the notch were determined at the failure instant, i.e. when the reaction force at the fixed end reaches the experimental failure load measured in the experimental test. As brittle behavior is assumed, failure load is considered as the maximum of the force-displacement curves. Figure 5 shows one of the finite element meshes corresponding to a notch tip radius of 1 mm.

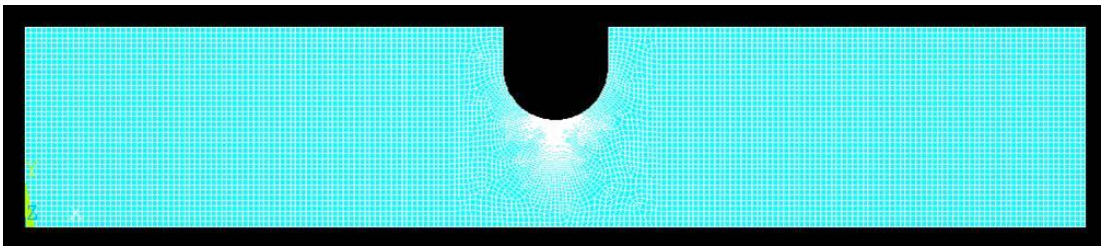

Figure 5. Example of one of the finite element meshes corresponding to a notch tip radius of 1 mm and the displacement histories applied.

The TCD with the Point Method (PM) was used as a failure criterion: failure occurs when the stress at a distance L/2 from the notch tip reaches a critical value σ_0:

$$\sigma\left(r=\frac{L}{2}\right)=\sigma_0 \qquad (1)$$

The TCD has four different approaches to obtain the critical parameters. The simplest methodology is the PM: it assumes that fracture occurs when the stress reaches the inherent strength (σ_0) at a certain distance from the defect tip (L/2). The critical stress σ_0 and the characteristic distance L are considered material constants that can be obtained from the intersection of the stress-distance curves corresponding to different notch tip radii [13].

2.5. Fracture toughness (K_{IC})

The results of the finite element analysis for each notch tip radii and sharp cracked specimens were used to calculate the fracture toughness. Fracture toughness of cracked specimens was obtained using Fracture Mechanics and the Theory of Critical Distances (TCD) has been used to evaluate the fracture toughness of notched samples. First, an apparent value of fracture toughness is calculated using the expression for each notch specimen [14]:

$$K_C^N = \frac{\sigma_{tip}}{2}\sqrt{\pi\rho} \qquad (2)$$

where K_C^N is the apparent fracture toughness, σ_{tip} is the stress at the crack tip and ρ is the tip notch radius. Both ρ and σ_{tip} are different for each specimen: the radius of the notch of each specimen was measured and σ_{tip} was calculated using the particular stress concentration factor. So, there were as many K_C^N as samples tested

Then, the apparent fracture toughness can be combined with the TCD theory (in the PM) to obtain an equivalent fracture toughness for each different tip radii [7]:

$$K_{IC} = K_C^N \frac{\left(1+\frac{2\rho}{L}\right)}{\left(1+\frac{\rho}{L}\right)^{3/2}} \qquad (3)$$

On the other hand, the value of fracture toughness was calculated using the sharp crack specimens and the linear elastic fracture mechanics expression:

$$K_{IC} = \sigma_{ROT} F(a/b)\sqrt{\pi a} \qquad (4)$$

where σ_{ROT} is the maximum stress, *a* is the crack length, *b* is the width of the specimen and *F(a/b)* is the shape factor given by [15]:

$$F\left(a/b\right) = 1.122 - 0.231\left(a/b\right) + 10.550\left(a/b\right)^2 - 21.710\left(a/b\right)^3 + +30.382\left(a/b\right)^4 \qquad (5)$$

2.6. Weibull statistical analysis

The presence of defects in the materials processed by additive manufacturing techniques, suggests the use of a probabilistic analysis of the failure load results. In this case, we have opted for an adjustment using the Weibull distribution. This function has been chosen since it has been widely used in materials that have defects, giving good results and for simplicity in its application. The expression used in this work corresponds to a Weibull distribution with three parameters. The cumulative failure probability (P_f) on which the distribution curve is based follows the next equation [16-18]:

$$P_{fail} = 1 - exp\left[-\left(\frac{K_{IC} - K_{min}}{K_0 - K_{min}}\right)^m\right] \qquad (6)$$

where K_{IC} is the fracture toughness for the selected failure probability (P_f), K_0 is a scale parameter located at the 63.2% cumulative failure probability level, *m* is the shape factor (Weibull modulus) and K_{min} is the lowest fracture toughness that would cause failure in this kind of samples, i.e. a threshold fracture toughness.

3. RESULTS AND DISCUSSION

3.1 Theory of critical distances parameters

Elastic stress fields calculated by finite element modelling were used to determine the TCD parameters. Fig.6 shows the stress-distance curves corresponding to nominal notch tip radii of 0.2 mm and 1 mm. The stress distributions used were those obtained for an average failure load value of all the samples tested with those nominal radii.

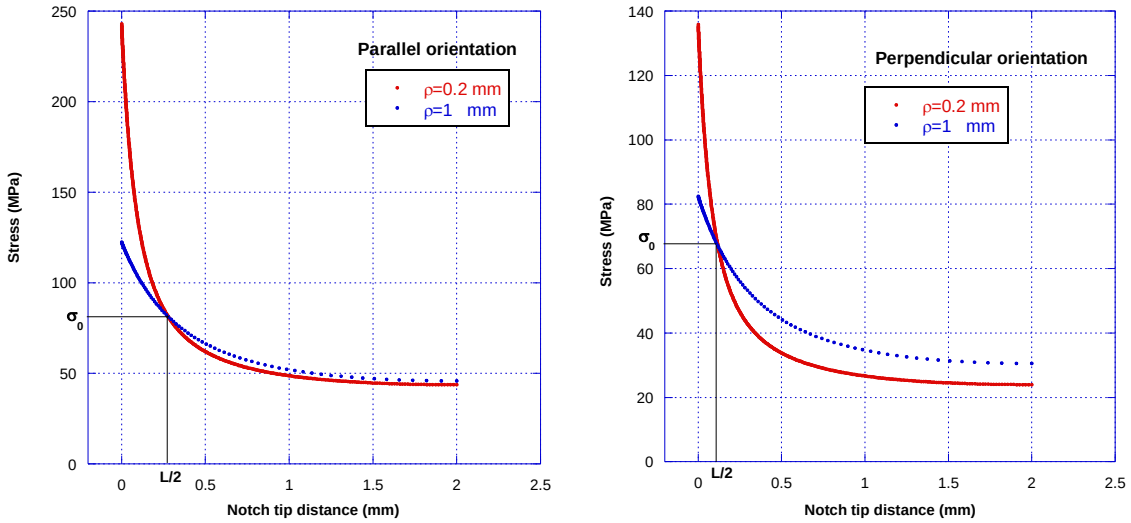

Figure 6. Stress - distance curves corresponding to extreme notch tip radii (the biggest tip radii, 1mm and the smallest, 0.2 mm) of parallel (left) and perpendicular (right) orientation samples.

These radii are the extreme cases analyzed and the values of the characteristic stress and the characteristic length can be obtained from the intersection between both stress-distance curves. Taking into account that experimentally the curves corresponding to different radii do not intersect at the same point, the choice of these extreme cases seems to be reasonable. The values obtained from the experiments and analyses done in this study were, are σ_0=67.2 MPa, and L=236 μm for the perpendicular orientation (90º), and σ_0=81.1 MPa, and L=560 μm for the parallel direction (0º).

3.2 Mechanical properties

Mechanical characterization of PA 12 manufactured by SLS manufacturing additive technique has been performed by tensile tests. The mean value of at least fifteen samples in each orientation are shown in Table 1.

Table 1. PA12 SLS manufactured mechanical properties

Property	Orientation 0º	Orientation 90º
Tensile stress	49 ± 2 MPa	34 ± 12 MPa
Young´s Modulus	1.60 ±0.15 GPa	1.55±0.15 GPa
Density	0.985 g/cm^3	0.982 g/cm^3

3.3 Failure loads

The experimental failure loads on the notched specimens vary for the different notch radii as shown in Figure 7. As expected, the fracture load increases with the notch tip radius, being cracked samples those exhibiting the lowest load at fracture point. The stress concentration increases as the radius decreases.

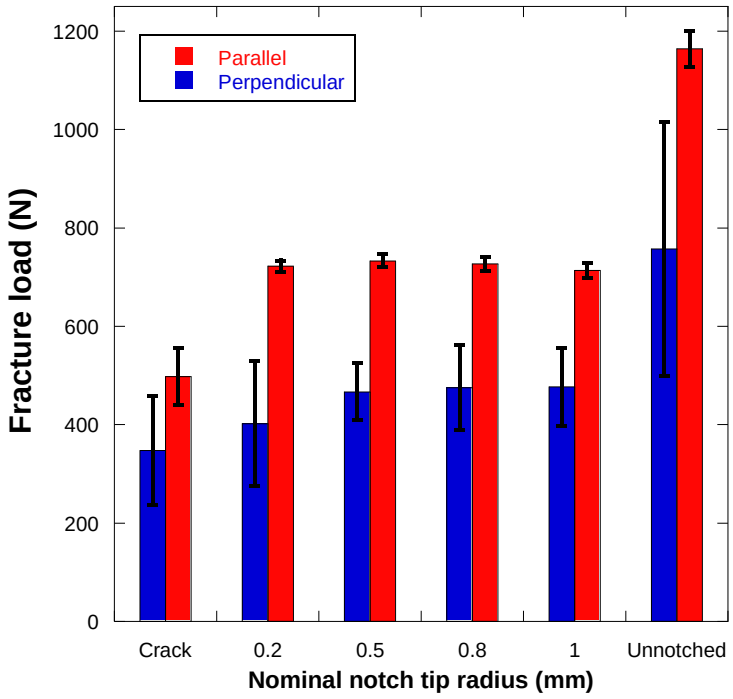

Figure 7. Failure loads of cracked and notched samples manufactured in parallel (0º) and perpendicular (90º) directions.

The results obtained show a high dispersion that has been associated with the existence of defects and the presence of un-melted particles. Figure 8 compares the load displacement curves obtained in one of the geometries tested for both orientations. Focused on each tip radius, an increase in the results dispersion can be appreciated in the samples with the manufacturing direction perpendicular to the applied load, i.e. in the 90º samples.

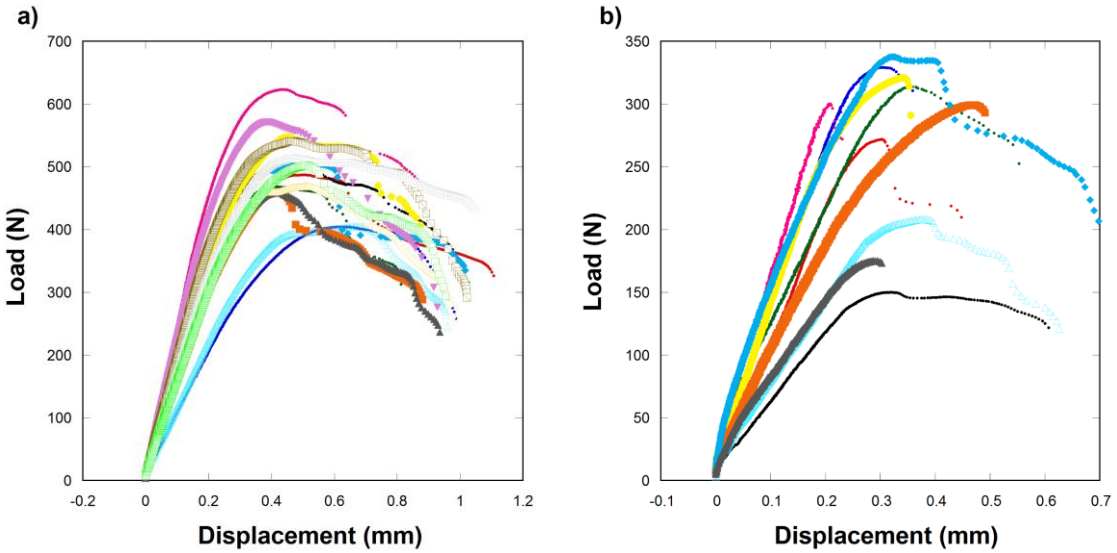

Figure 8. Force-displacement curves for cracked samples with the manufacturing direction a) parallel and b) perpendicular to the tensile load applied in the tests.

3.4 Fracture surfaces analysis

Experimental results show high dispersion, probably due to the presence of defects and un-melted particles. Figure 9 shows some micrographs corresponding to a smooth tensile specimen tested in the perpendicular orientation, where these evidences can be observed.

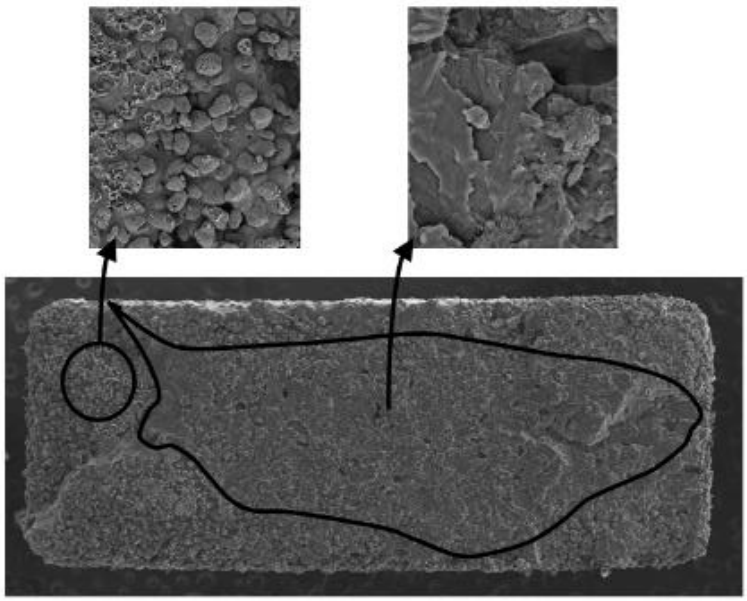

Figure 9. SEM micrographs of the fracture surface of a perpendicular orientated sample, where manufacturing defects can be appreciated.

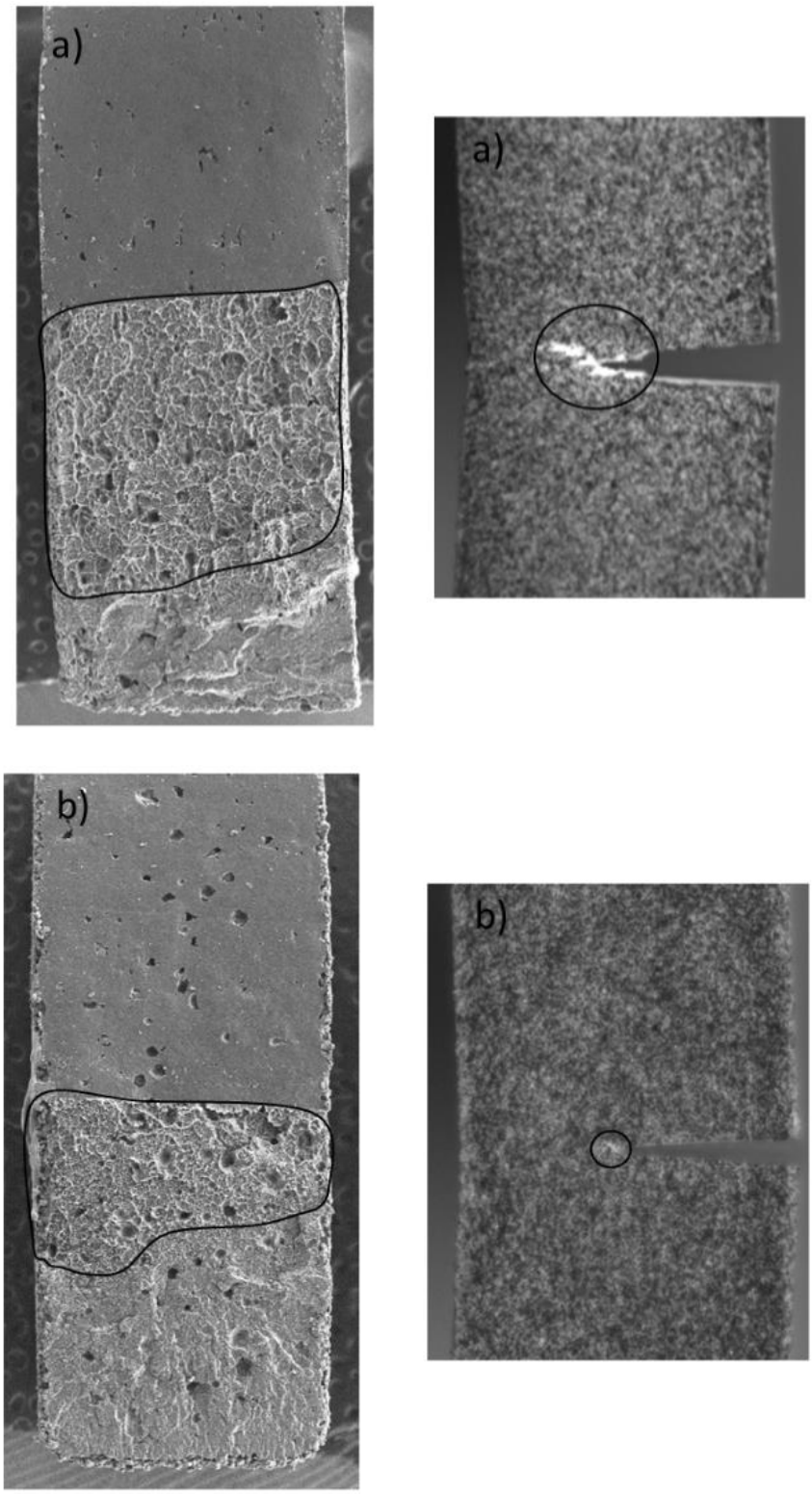

Figure 10. SEM images of the fracture surfaces and crack tip of a) parallel and b) perpendicular samples. In these images plastic deformed zone have been enhanced.

In Figure 10, fracture surfaces of the parallel (a) and perpendicular (b) samples are shown. Three zones can be observed: the notch zone, an intermediate area and a region of brittle fracture. The intermediate area may be associated with the non-linear behavior detected

in the load-displacement curves. Fracture surfaces in parallel samples presented larger non-linear zones, coinciding with the longer elongation at break.

3.5 Weibull statistical analysis

The fracture toughness values obtained for each orientation can be adjusted by a Weibull distribution function, as follows:

- Parallel orientation

$$P_{fail} = 1 - exp\left[-\left(\frac{K_{IC}-2.69}{3.35-2.69}\right)^{3.28}\right] \quad (7)$$

- Perpendicular orientation

$$P_{fail} = 1 - exp\left[-\left(\frac{K_{IC}-0.46}{2.22-0.46}\right)^{4.03}\right] \quad (8)$$

Figure 11 shows the cumulative probability, P_{fail}, versus fracture toughness, K_{IC}, for each orientation.

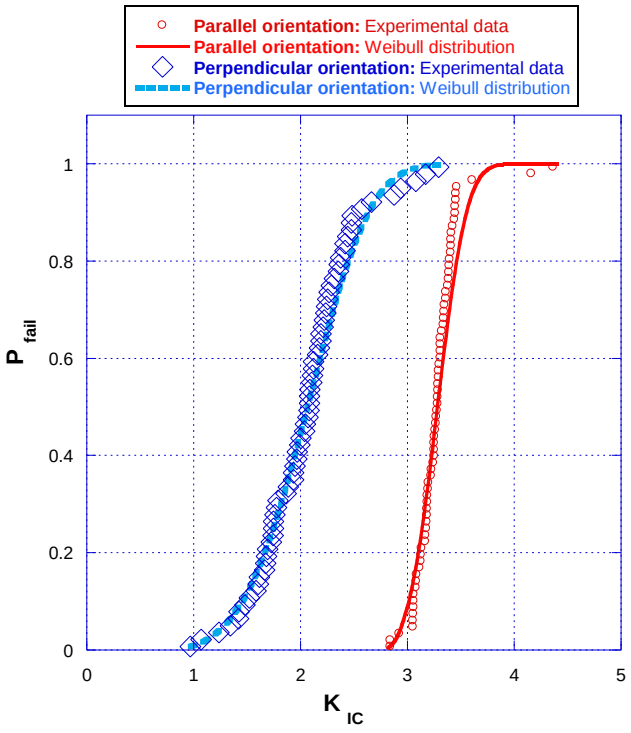

Figure 11. Comparison of Weibull distributions and experimental data for each specimen type: parallel (0°) and perpendicular (90°).

Weibull distributions were performed for each radius of the notched samples (Table 2) and also combining all the radii data transforming apparent fracture toughness into real fracture toughness through equation 3. Weibull parameters show that the distributions obtained for each radius independently or after combining all radii are very similar, which means consistency of the procedure used.

Table 2. Fracture toughness values obtained as Weibull parameter (K_0) for notched and cracked samples.

Type of sample	Notch tip radius ρ (mm)		K_0 parallel ($MPam^{1/2}$)	K_0 perpendicular ($MPam^{1/2}$)
Notched	0.2		3.13	2.24
	0.5		3.41	2.14
	0.8		3.35	2.01
	1		3.25	2.00
	All radii		3.38	2.01
Cracked			3.39	2.96
All samples			3.35	2.22

The TCD seems to be suitable to calculate the real fracture toughness from notched samples in this material SLS PA 12, showing only a deviation of 3% in the case of parallel orientation and 17% in the case of perpendicular orientation. This effect is probably due to the presence of manufacturing defects and lack of adhesion between the layers that weakens the sample in this direction.

4. CONCLUSIONS

This paper presents an analysis of the notch radius effect in SLS polyamide 12 specimens, and the application of the Theory of Critical Distances, in the Point method version, in order to validate their apparent fracture toughness predictions with the experimental results obtained from fracture tests with sharp crack specimens. The main conclusions obtained are the following:

- The manufacturing direction affected both the value of fracture toughness and tensile stress for the PA 12 studied.

- The TCD suitably reproduces values of fracture toughness obtained from notched samples of PA 12 manufactured by SLS. The approximation better fits the parallel manufacturing direction rather than the perpendicular.

- The samples manufactured with the layers perpendicular to the applied tensile force showed more scatter in the experimental results probably due to a higher amount of defects in the sample.

ACKNOWLEDGEMENTS

The authors of this work would like to express their gratitude to the Spanish Ministry of Economy and Competitiveness for the financial support of the project *DPI2016-80389-C2-1-R*.

REFERENCES

1. Forster A, Materials testing standards for additive manufacturing of polymer materials: State of the art and standards applicability, in *Additive Manufacturing Materials: Standards, Testing and Applicability*, 2015, p. 67-123.

2. Tofail SAM, Koumoulus EP, Bandyopadhyay A, Bose S, O´Donoghue L and Charitidis C. Aditive manufacturing: scientific and technological challenges, market uptake and opportunities. *Materials Today* 2018, 21 (1):22-37.

3. American Society for Testing Materials (ASTM), "F2792 - 12a : Standard Terminology for Additive Manufacturing Technologies," ASTM Standards, 2013.

4. Goodridge R, Tuck C and Hague R, Laser sintering of polyamides and other polymers, *Progress in Materials Science* 2012, 57 (2): 229-267.

5. Obsta P, Launhardta M, Drummera D, Osswaldb PB and Osswaldc TA. Failure criterion for PA12 SLS additive manufactured parts. *Additive Manufacturing*, 2018, 21: 619-627.

6. Cicero S, Madrazo V, Carrascal I and Cicero R, Assessment of notched structural components using failure assessment diagrams and the theory of critical distances, *Engineering Fracture Mechanics* 2011, 78:2809-2825.

7. Taylor D, *The Theory of Critical Distances: A New Perspective in Fracture Mechanics*, UK: Elsevier, 2007.

8. Muniz-Calvente M, Blasón S, Correia J, Cicero S, de Jesus A and Fernández Canteli A, A probabilistic approach to derive the apparent fracture toughness of notched components based on TCD, in *International Symposium on Notch Fracutre*, Santander (Cantabria, Spain), 2017.

9. L. Susmel, D. *Taylor*. The Theory of *Critical Distances* to estimate finite lifetime of notched components subjected to constant and variable amplitude torsional loading. Engineering Fracture Mechanics, 2013, 98; pp. 64-79.

10. L. Susmel, D. *Taylor*. The Theory of *Critical Distances* as an alternative experimental strategy for the determination of KIc and ΔKth. Engineering Fracture Mechanics, 2010, 77 89), pp. 1492-1501.

11. Stichel T, Frick T, Laumer T, Tenner F, Hausotte T, Merklein M and Schmidt M, A Round Robin study for Selective Laser Sintering of polyamide 12: Microstructural origin of the mechanical properties, *Optics and Laser Technology* 2017, 89: 31-40.

12. American Society for Testing Materials (ASTM), "D638-03 : Standard test method for tensile properties of plastics," ASTM standards, 2003.

13. Taylor D. The theory of Critical Distances. *Engineering Fracture Mechanics* 2008, 75 (7) :1696-1705.

14. G. Glinka. Calculation of Inelastic Notch-tip Strain-stress Histories Under Cyclic Loading. Engineering Fracture Mechanics, 1985, 22 (5), p. 839-854.

15. Tada H, Paris P and Irwin G, *The Stress Analysis of Cracks Handbook*, Ney York: The American Society of Mechanical Engineers (ASME-Press), 2000.

16. Rinne H, *The Weibull Distribution: A Handbook*, U.S.: CRC Press, 2009.

17. Weibull W, *A Statistical Distribution Function of Weibull, ASME Journal of Applied Mechanics, 1951*, p. 293-297.

18. Weibull W, A Statistical Distribution Function of Wide Applicability (Discussion), *ASME Journal of Applied Mechanics, 1952*, p. 233-234.